Cubic ZnO films obtained at low pressure by molecular beam epitaxy*

Wang Xiao-Dan(王小丹), Zhou Hua(周 华), Wang Hui-Qiong(王惠琼)†, Ren Fei(任 飞), Chen Xiao-Hang(陈晓航), Zhan Hua-Han(詹华瀚), Zhou Ying-Hui(周颖慧), and Kang Jun-Yong(康俊勇)

Key Laboratory of Semiconductors and Applications of Fujian Province, Department of Physics, Xiamen University, Xiamen 361005, *China*

(Received 30 March 2015; revised manuscript received 3 June 2015; published online 20 July 2015)

A zinc oxide thin film in cubic crystalline phase, which is usually prepared under high pressure, has been grown on the MgO (001) substrate by a three-step growth using plasma-assisted molecular beam epitaxy. The cubic structure is confirmed by *in-situ* reflection high energy electron diffraction measurements and simulations. The x-ray photoelectron spectroscopy reveals that the outer-layer surface of the film (less than 5 nm thick) is of ZnO phase while the buffer layer above the substrate is of ZnMgO phase, which is further confirmed by the band edge transmissions at the wavelengths of about 390 nm and 280 nm, respectively. The x-ray diffraction exhibits no peaks related to wurtzite ZnO phase in the film. The cubic ZnO film is presumably considered to be of the rock-salt phase. This work suggests that the metastable cubic ZnO films, which are of applicational interest for p-type doping, can be epitaxially grown on the rock-salt substrates without the usually needed high pressure conditions.

Keywords: ZnO film, rock-salt structure, molecular beam epitaxy, reflection high energy electron diffraction

PACS: 71.55.Gs, 81.15.–z, 68.55.–a, 61.05.jh **DOI:** 10.1088/1674-1056/24/9/097106

1. Introduction

ZnO, as a II–VI semiconductor, being widely used in many scientific and industrial areas such as piezoelectric transducers, optical waveguides, acousto-optic media, transparent conductive electrodes, conductive gas sensors, varistors, and solar cells,[1–6] has a hexagonal wurtzite structure (B4) under ambient conditions. Its metastable cubic structures, including rock-salt (RS) structure (B1) and zinc-blende (ZB) structure (B3), are usually obtained under high pressure.[7–10] The p-type doping of ZnO, which is difficult in the hexagonal B4 structure, can be realized in both cubic RS-B1 structure and cubic ZB-B3 structure.[11,12] The ZB-B3 structure may have additional advantages of reducing the spontaneous polarization.[12] Lots of researchers have experimentally demonstrated that it is rather difficult to obtain the cubic ZnO films grown directly on the substrates.[12,13] So far, only a few experimental studies have been carried out on cubic RS-ZnO in ordinary conditions. Decremps *et al.*[14] reported a study on cubic ZnO nanocrystallites and showed that the trapping of cubic ZnO was achieved at ambient conditions. Kunisu *et al.*[15] reported the fabrication of RS-type ZnO thin films by low-level alloying with MgO. More studies about pure RS-ZnO films are required. The growth of high-quality zinc-blende ZnO is also of challenge due to the unclear underlying mechanism of the ZB formation.[16] In a word, it is of great difficulty as well as importance to obtain the cubic ZnO thin films in both RS-B1 structure and ZB-B3 structure. Inspired by the fact that ZnO thin films in cubic ZB phase have only been obtained in epitaxy growth on cubic substrates,[12] we explore the fabrication of cubic RS-ZnO thin films on cubic RS-MgO (001) substrates by molecular beam epitaxy. It is worth mentioning that cubic substrates such as MgO could also be used to grow hexagonal wurtzite ZnO films,[17–19] i.e., not just the cubic epitaxial ZnO films. Therefore, it would be interesting to explore the growth mechanisms of different ZnO phases on the top of the same MgO substrate. Moreover, the integration of ZnO and MgO is also of interest in terms of band gap engineering.[20]

2. Experiments

First the commercial single-crystal MgO substrates with ⟨001⟩ orientation were cleaned successively in acetone and ethanol using an ultrasonic bath. The cubic ZnO films were then grown on the MgO (001) substrates by plasma-assisted molecular beam epitaxy (p-MBE) using a three-step approach, including an annealing process (step 1), a buffer-layer growth process (step 2), and a film-growth process (step 3) in sequence. In step 1, the substrate was annealed at 500 °C for 60 min with the oxygen partial pressure maintained at 5×10^{-5} mbar and the power of the radio frequency plasma source set to 250 W. In step 2, a buffer layer was grown in 20 min with a substrate temperature of 200 °C, a zinc temperature of

*Project supported by the National Natural Science Foundation of China (Grant Nos. 11204253, U1232110, U1332105, 61227009, and 91321102), the Fundamental Research Funds for Central Universities, China (Grant No. 2013SH001), and the National High Technology Research and Development Program of China (Grant No. 2014AA052202).

†Corresponding author. E-mail: hqwang@xmu.edu.cn

© 2015 Chinese Physical Society and IOP Publishing Ltd

310 °C, an oxygen partial pressure of 1.5×10^{-5} mbar, and 100 W power of the radio frequency plasma source. In step 3, the film was grown in 60 min with a substrate temperature of 420 °C, a zinc source temperature of 310 °C, an oxygen partial pressure of 1.5×10^{-5} mbar, and an oxygen plasma power of 100 W. The thickness of the film was about 19 nm as examined by a variable angle spectroscopic ellipsometer (VASE). The cubic-ZnO structure was identified by *in-situ* reflection high energy electron diffraction (RHEED) and the corresponding RHEED simulations using the MATLAB program[21] according to the diffraction theory, as well as the x-ray diffraction (XRD) using a Cu anode ($\lambda_{K\alpha 1} = 1.54056$ Å). The chemical compositions and the band gap features of the thin films were probed by x-ray photoelectron spectroscopy (XPS) and transmission spectrum, respectively.

3. Results and discussion

Figure 1 shows the RHEED patterns featuring the three steps of growth, captured along the $[100]_{ZnO}$ and $[110]_{ZnO}$ directions respectively. Figures 1(a) and 1(b) are the RHEED patterns of the MgO (001) substrate after the 60-min annealing. The streaky patterns with clear Kikuchi lines indicate a well-ordered substrate surface, which is a prerequisite for high-quality epitaxy. The RHEED patterns of the ZnO buffer layer after 20-min deposition are shown in Figs. 1(c) and 1(d). In these two figures, the sharp and streaky lines completely disappear and are replaced by spotty patterns, which are the indications of the 3D island morphology. The three-dimensional growth at the initial stage in the 20-min-buffer-layer growth process maintains the cubic structure, with the lattice constant being almost the same as that of the substrate, as shown by the aligned red lines (L1–L4) in Fig. 1. It can be explained by the fact that numerous Mg atoms diffuse into the ZnO film during the buffer layer growth because of the lower evaporation energy for Mg atoms on the MgO (001) surface,[22] which results in the formation of a ZnMgO film with cubic structure, as confirmed by the XPS results in the later discussion. What is rather interesting is that, as shown in Figs. 1(e) and 1(f), the RHEED patterns taken from the film sample after the 60-min growth are nearly identical to those from the buffer layer, which strongly reveals that the ZnO film is of cubic structure. It is noticed that the distance between L3 and L4 in Fig. 1(b) is slightly larger than that between L5 and L4 in Fig. 1(f). These results indicate that the lattice constant of the ZnO film with cubic structure is slightly larger than that of the cubic MgO substrate. In fact, according to the measured ratio ($d_1/d_2 \approx 1.06$, d_1 represents the distance between L3 and L4, d_2 represents the distance between L5 and L4), we estimate the lattice constant of the as-grown film to be about 4.46 Å, where the experimental result of 4.21 Å is used as the lattice constant of MgO. It is worth pointing out that our attempt to improve the quality of the HT-ZnO layer by employing a low temperature grown ZnO buffer layer (LT-ZnO) following the report in Ref. [23] was not successful, i.e., the RHEED patterns retained spotty during the growth of HT-ZnO, showing the 3D island growth mode.

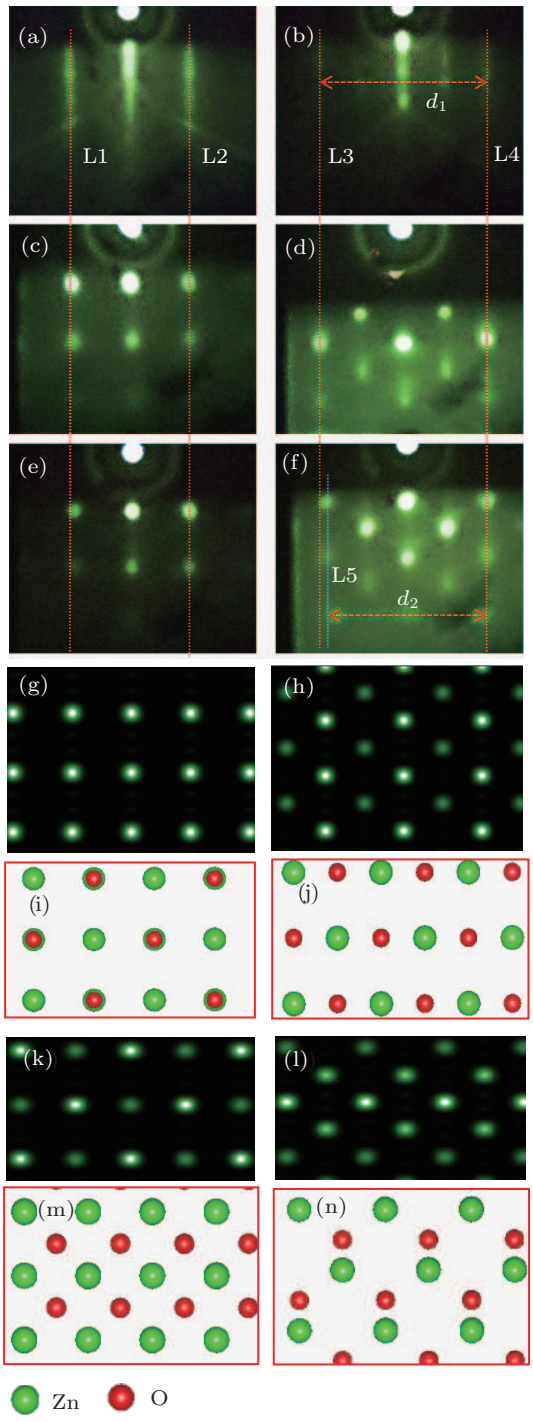


Fig. 1. (color online) RHEED patterns captured after substrate annealing, buffer-layer growth, and film growth, along the [100] ((a), (c), (e)) and [110] ((b), (d), (f)) azimuths, respectively. Panels (i) and (j) are the side views of the atomic model of rock-salt ZnO along [100] and [110] directions, respectively, with the corresponding simulated RHEED patterns shown in panels (g) and (h). Panels (m) and (n) are the side views of the atomic model of zinc-blende ZnO along [100] and [110] directions, respectively, with the corresponding simulated RHEED patterns shown in panels (k) and (l).

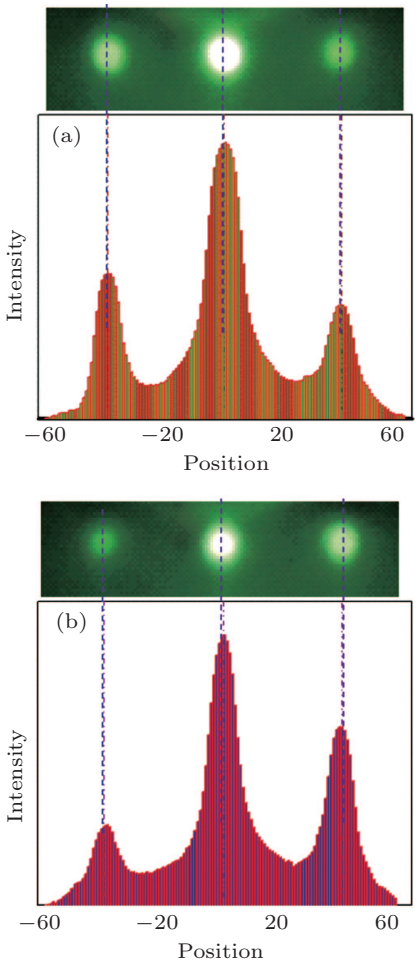


Fig. 2. (color online) The diffraction intensity profiles from the horizontal direction of the RHEED patterns (using the top three spots) in (a) Fig. 1(c) and (b) Fig. 1(e).

As the MgO substrate is of rock-salt structure, and the evolution of the RHEED patterns of the buffer ZnO layer and the grown ZnO film follows a similar pattern, the grown ZnO film is presumed to be of the rock-salt structure as well. Figures 1(g) and 1(h) show the simulated RHEED patterns of the rock-salt ZnO overlayers along the $[100]_{ZnO}$ and $[110]_{ZnO}$ azimuths, respectively, and the corresponding atomic models are presented in Figs. 1(i) and 1(j). Four atomic layers in the top surface are included in the simulation to reflect the 3D growth mode. For comparison, the RHEED patterns of the ZnO surface with the zinc-blende structure along the $[100]_{ZnO}$ (Fig. 1(k)) and $[110]_{ZnO}$ (Fig. 1(l)) azimuths are also simulated, and the corresponding atomic models are presented in Figs. 1(m) and 1(n). The RHEED patterns of the as-grown film (Figs. 1(e) and 1(f)) are highly compatible with the simulated RHEED patterns of the cubic structures (either rock-salt ZnO or zinc-blende ZnO is possible if the variation of the intensity among the spots is not considered). As the RHEED spot intensity is also an indication of the fine structure, which is related to the structural form factor, the intensity modulation of the three consecutive points (horizontal direction) in the RHEED pattern of the buffer ZnO layer (Fig. 1(c)) is analyzed (as shown in Fig. 2(a)), and compared to the corresponding intensity modulation profile (Fig. 2(b)) in the RHEED pattern of the grown ZnO film (Fig. 1(e)). The similarity of the intensity profiles in Figs. 2(a) and 2(b) indicates the similarity of the atomic structure between the MgZnO buffer layer and the ZnO overlayer. As the MgZnO buffer layer is determined to extend the symmetry from the rock-salt MgO substrate, the phase of the ZnO film is therefore considered to be rock-salt as well. Furthermore, the calculated lattice constant of 4.46 Å for the grown cubic ZnO film as mentioned above is in good agreement with the previous report.[3] This demonstrates the feasibility to acquire cubic ZnO films at a low oxygen partial pressure by p-MBE.

In order to investigate the electronic structure and the chemical composition of the thin film, XPS spectra were captured after growth and after being etched using the Argon ion beam, as illustrated by the dark and red curves in Fig. 3, respectively. The thickness of the part etched by the argon source is estimated to be about 5 nm. As the thickness of the whole film is measured to be about 19 nm, the buffer layer of ZnMgO is estimated to be about 14 nm. The corresponding XPS survey scan spectra of the ZnO thin film before and after etching are shown in Fig. 3(a), which display the Mg-2p, Ar-2p, C-1s, Zn-LMM, O-1s, Zn-2p3/2, and Zn-2p1/2 feature peaks. The existence of the C-1s peaks before the etching is due to the slight contamination of the film and the emergence of the Ar-2p peaks after the etching is attributed to the use of argon as the etching ion source. Most importantly, the weak peak of Mg-2p before the etching (Fig. 3(b)) indicates the ignorable Mg component in the grown film. In other words, the top layer of the film (less than 5 nm thick) is cubic ZnO, rather than ZnMgO. Meanwhile, the fact that the Mg component increases dramatically after the etching (Fig. 3(b)) with only a slight decrease of the Zn component (Figs. 3(c) and 3(d)) suggests that the buffer layer is MgZnO. Interestingly, the Zn-2p XPS peak shifts to a slightly higher binding energy after the etching (as shown in Fig. 3(c)). This could be attributed to a slight change of the chemical environment before and after the etching, as the top layer of the film is cubic ZnO, while the lower layer is cubic ZnMgO. This result can be further confirmed by the Zn LMM AES spectra, which change from two peaks to one peak after the etching (as shown in Fig. 3(d)). Figure 3(e) shows the O 1s XPS spectra with fitting results using a Gaussian function. Two bonding configurations are identified before the etching, namely, M–O (Zn or Mg–O) bond at 529.3 eV and OH^- bond at 531.3 eV, and the latter disappears after the etching. The band-gap feature of the film was also probed using the transmission spectrum, as shown in Fig. 4(a),

which can also be used to estimate the phase of the film. The transmission spectrum from the film shows two slopes, one at the wavelength of about 390 nm, and the other at the wavelength of about 280 nm, which correspond to the band edges of the cubic ZnO film and ZnMgO film, respectively. This is consistent with the RHEED patterns and the XPS data shown above. Besides, the corresponding XRD results (red line) of the film shown in Fig. 4(b) exhibit almost the same pattern as that for the cubic rock-salt MgO substrate (blue line) without any peaks related to the wurtzite ZnO structure.

As demonstrated, a possible rock-salt phase ZnO has been grown on the top of the cubic MgO substrate. As the rock-salt structure of ZnO is metastable and is usually prepared or transformed from the wurtzite phase prepared under very high pressure, the question arises as to why the rock-salt ZnO phase could be obtained under low pressure in our work. It could be attributed to the three-step growth. After the annealing of the substrate, the buffer layer of ZnMgO is prepared with a three-dimensional growth under the condition of extremely low flux and growth temperature to maintain the cubic structure of the substrate. When the substrate temperature is increased for the later growth stage, the diffusion of the Mg atoms from the substrate to the film is limited due to the relatively thick buffer layer, which thus guarantees the growth of ZnO without Mg during the lattice epitaxy of the cubic rock-salt structure.

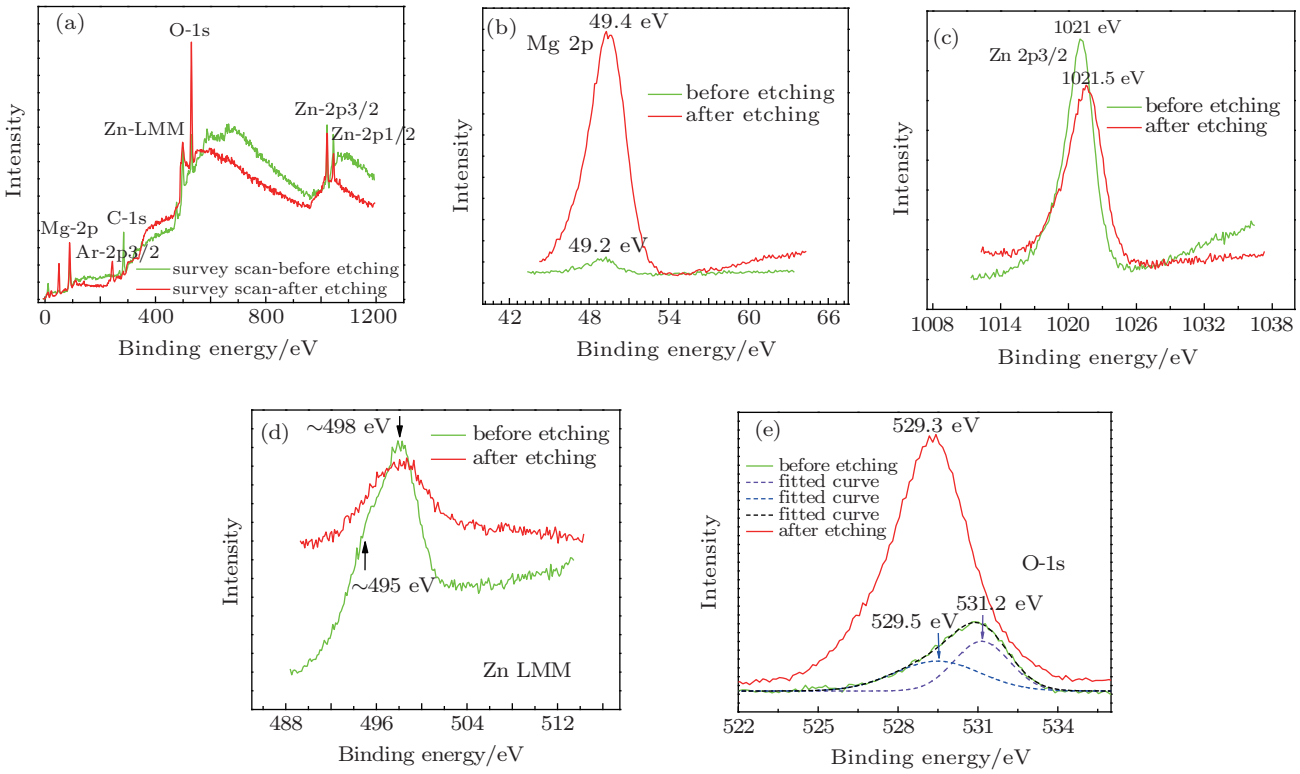


Fig. 3. (color online) X-ray photoelectron spectra of the grown film before (green) and after (red) etching: (a) the survey scan, (b) Mg 2p, (c) Zn 2p3/2, (d) Zn LMM, and (e) O 1s.

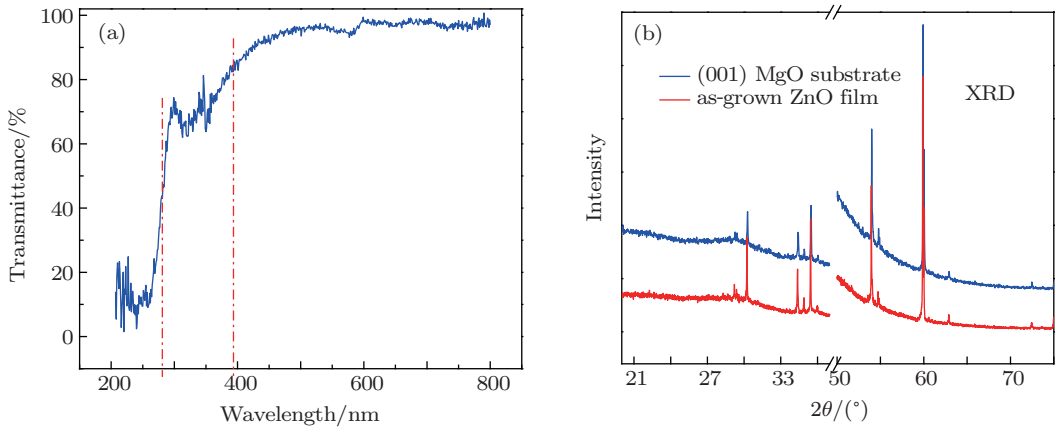


Fig. 4. (color online) (a) UV–vis transmission spectrum of the ZnO film with the two band edge transmissions at the wavelengths of 280 nm and 390 nm, respectively. (b) XRD patterns of the MgO substrate and the ZnO film.

4. Conclusion

The growth of a cubic ZnO film (with a possible rock-salt phase) on the MgO (001) substrate has been experimentally demonstrated. The RHEED patterns verify the cubic structure of the film surface. The chemical composition and the structure of the outer layer of ZnO and the buffer layer of MgZnO are further confirmed by XPS and transmission spectrum. This work shows the possibility to grow metastable rock-salt ZnO films under low pressure conditions.

References

[1] Robert T 2014 *Prog. Cryst. Growth* **60** 1

[2] Hwang D K, Oh M S, Lim J H and Park S J 2007 *J. Phys. D: Appl. Phys.* **40** R387

[3] Özgür Ü, Alivov A I, Liu C, Teke A, Reshchikov M A, Do an S, Avrutin V, Cho S J and Morkoc H 2005 *J. Appl. Phys.* **98** 041301

[4] Sanchez-Valencia J R, Alcaire M, Romero-Gómez P, Macias-Montero M, Aparicio F, Borras A, Gonzalez-Elipe A and Barranco A 2014 *J. Phys. Chem. C* **118** 9852

[5] Bang J, Kim Y S, Park C H, Gao F, and Zhang S B 2014 *Appl. Phys. Lett.* **104** 252101

[6] Sougata P, Torben J T, Michael H and Eckhard P 2013 *Phys. Rev. B* **87** 085445

[7] Kim S K, Jeong S Y and Cho C R 2003 *Appl. Phys. Lett.* **82** 562

[8] Santosh M B 2012 *Appl. Phys. Lett.* **100** 072101

[9] Mahlaga P M and Daniel P 2011 *Phys. Rev. B* **84** 094110

[10] Ni H Q and Ren Z M 2002 *J. Appl. Phys.* **91** 1339

[11] Liu H Z, Tse J S andMao H K 2006 *J. Appl. Phys.* **100** 093509

[12] Ashrafi A and Jagadish C 2007 *J. Appl. Phys.* **102** 071101

[13] Yoo Y Z, Osaka Y, Fukumura T, Jin Z, Kawasaki M, Koinuma H, Chikyow T, Ahmet P, Setoguchi A and Chichibu S F 2001 *Appl. Phys. Lett.* **78** 616

[14] Martínez P L, Muñoz A N, Muñoz A S and Zelaya A O 2015 *Mater. Lett.* **139** 63

[15] Kunisu M, Tanaka I, Yamamoto T, Suga T and Mizoguchi T 2004 *J. Phys.: Condens. Matter* **16** 3801

[16] Decremps F, Piellicer-Porres J, Datchi F, Itie J P, Polian A and Baudelet F 2002 *Appl. Phys. Lett.* **81** 4820

[17] Zhou H, Wang H Q, Wu L, Zhang L, Kisslinger K, Zhu Y, Chen X, Zhan H and Kang J 2011 *Appl. Phys. Lett.* **99** 141917

[18] Zhou H, Wang H Q, Liao X X, Zhang Y, Zheng J C, Wang J O, Muhemmed E, Qian H J, Ibrahim K, Chen X, Zhan H and Kang J 2012 *Nanoscale Res. Lett.* **7** 184

[19] Zhou H, Wang H Q, Li Y, Li K, Kang J, Zheng J C, Jiang Z, Huang Y, Wu L, Zhang L, Kisslinger K and Zhu Y 2014 *ACS Appl. Mater. Interfaces* **6** 13823

[20] Anderson J and Chris G V D W 2009 *Rep. Prog. Phys.* **72** 126501

[21] Wang K K and Smith R A 2011 *Comput. Phys. Commun.* **182** 2208

[22] Geneste G, Morillo J and Finocchi F 2005 *J. Chem. Phys.* **122** 174707

[23] Choa M W, Haradaa C, Suzukia H, Minegishia T, Yao T, Koc H, Maedad K and Nikurad I 2005 *Supperlattice Microst.* **38** 349